Dynamic modal characteristics of transverse vibrations of cantilevers of parabolic thickness

Dumitru I. Caruntu *

University of Texas-Pan American, Mechanical Engineering Department, Edinburg, TX 78541, USA

A B S T R A C T

This paper deals with free transverse vibrations of nonuniform homogeneous beams. Cantilevers of rectangular (or elliptical) cross-section with parabolic thickness variation, and cantilevers of circular cross-section with parabolic radius variation, are considered. Factoring their fourth order differential equations of transverse vibrations into a pair of second order differential equations leads to general solutions in terms of hypergeometric functions. Exact natural frequencies and exact mode shapes are reported for sharp parabolic cantilevers of various dimensionless lengths.

© 2008 Elsevier Ltd. All rights reserved.

1. Introduction

Numerous papers have been published on transverse vibrations of nonuniform beams due to their relevance to aeronautical, mechanical, and civil engineering. Yet, analytical solutions are available only for a few particular types of cross-section variations. These solutions are important since "it is difficult to draw general conclusions about the behavior of a system using only numerical methods" (Rao, 2004). Such analytical solutions in terms of (a) orthogonal polynomials Caruntu (2007, 2005, 1996), (b) Bessel functions (Auciello and Nole, 1998; De Rosa and Auciello, 1996; Craver and Jampala, 1993; Goel, 1976; Sanger, 1968; Mabie and Rogers, 1968; Conway and Dubil, 1965; Conway et al., 1964; Cranch and Adler, 1956), (c) hypergeometric series (Storti and Aboelnaga, 1987; Wang, 1967), and (d) power series by Frobenius method (Chaudhari and Maiti, 1999; Naguleswaran, 1995, 1994a,b; Wright et al., 1982), have been reported in the literature. Abrate (1995) presented a method in which the equation of motion of a class of nonuniform beams is transformed into one of uniform beams. Most of the investigated nonuniform beams of circular and/or rectangular cross-section were linearly tapered, but other cross-section variations were also considered. Circular cross-section has been considered for (a) truncated beams (De Rosa and Auciello, 1996; Naguleswaran, 1994a; Sanger, 1968; Mabie and Rogers, 1968; Conway et al., 1964), (b) beams of one end sharp (Caruntu, 2007; Naguleswaran, 1994b; Cranch and Adler, 1956), and (c) both ends sharp (Caruntu, 2007; Cranch and Adler, 1956). Rectangular cross-section has been considered for (a) beams of constant width (Naguleswaran, 1994b; Goel, 1976; Sanger, 1968; Mabie and Rogers, 1968; Conway and Dubil, 1965), (b) beams of constant thickness (Chaudhari and Maiti, 1999; Wright et al., 1982; Cranch and Adler, 1956), and (c) pyramids (Auciello and Nole, 1998; De Rosa and Auciello, 1996; Craver and Jampala, 1993; Goel, 1976; Sanger, 1968; Mabie and Rogers, 1968; Conway et al., 1964; Cranch and Adler, 1956). Of rectangular cross-section papers, (a) few were dedicated to beams of one end sharp (Caruntu, 2007; Naguleswaran, 1995, 1994a,b; Wright et al., 1982; Cranch and Adler, 1956), and (b) only two to the case of both ends sharp Caruntu (2007), Cranch and Adler (1956); (c) all others being dedicated to truncated beams. Width varying with any

---

* Tel.: +1 956 381 2079; fax: +1 956 381 3527.
  E-mail addresses: caruntud@utpa.edu, caruntud2@asme.org, dcaruntu@yahoo.com.

positive power of the longitudinal coordinate has been considered along with (a) constant thickness (Naguleswaran, 1995), (b) linear thickness (Sanger, 1968; Cranch and Adler, 1956), and (c) any positive power variation of thickness (Wang, 1967). Beams of parabolic thickness variation with particular boundary conditions and solutions in terms of orthogonal polynomials have been reported as well (Caruntu, 2007, 1996). Beams of exponential thickness and constant width were presented by Ece et al. (2007), and constant thickness and exponential width by Cranch and Adler (1956). An asymptotic approach for transverse vibrations of variable section beams has been reported by Firouz-Abadi et al. (2007). A recent mathematical investigation, Anderson and Hoffacker (2006), was dedicated to the existence of solutions of cantilever beam problem. As one can see there is a continuous effort in studying one dimensional continuous systems.

Cantilevers of parabolic thickness variation are important for studies regarding geometry influence on different phenomena. Cantilevers in general are key structures in many engineering applications. In particular they are extensively used as resonator sensors. Cantilever structures are integral parts of microelectromechanical (MEMS) biosensors for the detection of airborne virus particles (Johnson et al., 2006), and resonant nanoelectromechanical systems (NEMS) for a new class of ultra fast, highly sensitive devices (Cimalla et al., 2007). Results regarding nonuniform cantilevers of particular geometry used as resonator sensors have been already reported in the literature. For instance Turner and Wiehn (2001) considered the dynamics of atomic force microscope (AFM) cantilevers in terms of flexural vibrations. They investigated the sensitivity of a nonuniform cantilever beam (triangular with constant width) against a uniform cantilever, and found that for values of a studied parameter (the normal contact stiffness relative to the stiffness of the cantilever) greater than 100, the overall sensitivity of the triangular cantilever is greater than or equal to that of the uniform beam. The fact that nonuniform cantilevers can be, under specific circumstances, more sensitive than uniform cantilevers is an important result.

To the author's best knowledge, there are virtually no dynamic modal characteristics available in the literature for transverse vibrations of cantilevers of parabolic thickness. This paper aims to fill this gap by presenting the general solution of the differential equation of transverse vibrations of parabolic cantilevers, and the exact natural frequencies and exact mode shapes for the boundary value problems of sharp parabolic cantilevers. This paper presents a different approach and consequently different results than those reported by Caruntu (2007) who reported the class of beams and plates whose boundary value problems can be reduced to an eigenvalue singular problem of orthogonal polynomials. In the work of Caruntu (2007) the natural frequencies and the mode shapes (which were Jacobi polynomials) resulted directly, without any frequency equation to be solved, from the eigenfunctions and eigenvalues of orthogonal polynomials reported by Caruntu (2005). In this work, the fourth order differential equation of motion is factored into a pair of second order differential equations. General solution in terms of hypergeometric functions, and frequency equation resulting from cantilever boundary conditions, are reported. The exact natural frequencies and exact mode shapes are found for sharp parabolic cantilevers by solving the frequency equation.

This paper falls in the category of analytical methods and modeling for linear vibration, benchmark solutions. Results reported in this paper, along with already reported data for cantilevers linearly tapered (Cranch and Adler, 1956) and uniform cantilevers (Timoshenko et al., 1974) provide the necessary information for studies on geometry influences on free, forced, linear and/or nonlinear vibrations of such cantilevers. In particular the results of this paper are useful for studies on mass deposition sensitivity of resonator sensors.

2. Transverse vibration of nonuniform Euler–Bernoulli beams

Euler–Bernoulli differential equation of transverse vibrations of nonuniform beams is given by

$$\frac{d^2}{dx^2}\left[EI^*(x)\frac{d^2y(x)}{dx^2}\right] - \rho_0\omega^2 A^*(x)y(x) = 0, \quad x_1 < x < \ell, \tag{1}$$

where $y(x)$ is the transverse displacement, $A^*(x)$ and $I^*(x)$ are the area and moment of inertia of current cross-section, respectively; E, ρ_0 and ω are Young modulus, mass density, and natural frequency, respectively; x is the current longitudinal coordinate of the beam, and x_1 and ℓ are the coordinates of the fixed end and the free end of the beam, respectively, Fig. 1, where $|x_1| < \ell$. Using the variable changing

$$x = \xi\ell, \quad \frac{d}{dx} = \frac{1}{\ell}\cdot\frac{d}{d\xi}, \tag{2}$$

where ξ is the current dimensionless longitudinal coordinate of the beam, the dimensionless equation of transverse vibrations of nonuniform Euler–Bernoulli beams is obtained as follows:

$$\frac{1}{A(\xi)}\frac{d^2}{d\xi^2}\left[I(\xi)\frac{d^2y(\xi)}{d\xi^2}\right] - \bar{\omega}^2 y(\xi) = 0, \quad \xi_1 < \xi < 1, \tag{3}$$

where $A(\xi)$ and $I(\xi)$ are the dimensionless cross-section area and moment of inertia, ξ_1 is the dimensionless coordinate of the fixed end, and $\bar{\omega}$ is the dimensionless natural frequency given by

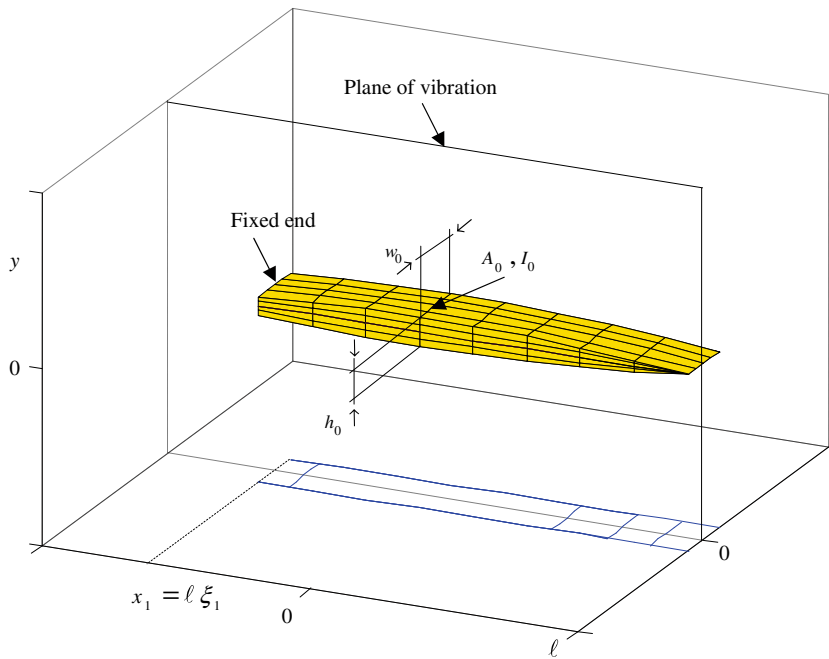$$\bar{\omega} = \omega\ell^2\sqrt{\frac{\rho_0 A_0}{EI_0}}. \tag{4}$$

Fig. 1. Cantilever of rectangular cross-section, parabolic thickness $h^* = h_0(1 - \xi^2)$, constant width $w^* = w_0$, and sharp end.

The reference cross-section area and moment of inertia, A_0 and I_0, are considered at the longitudinal coordinate $\xi = 0$ (or $x = 0$), Fig. 1.

3. Beam of rectangular cross-section and parabolic thickness

3.1. Differential equation

Consider a beam of rectangular cross-section, constant width $w^*(x)$, and parabolic thickness $h^*(x)$, Fig. 1, as follows:

$$w^*(x) = w_0 = \text{constant}, \quad h^*(x) = h_0\left(1 - \frac{x^2}{\ell^2}\right), \quad x_1 < x < \ell, \tag{5}$$

One can notice that the origin of the x axis is the midpoint of the complete beam (sharp at both ends, $-\ell < x < \ell$), and ℓ is half of the complete beam length. The complete beam is not investigated in this paper. It has been investigated by Caruntu (2007). The complete beam was mentioned just to indicate the location of the origin of the x axis. Using the variable changing given by Eq. (2), the current width w^*, thickness h^*, cross-section area A^*, and moment of inertia I^* can be written as

$$w^* = w_0 \cdot w(\xi), \quad h^* = h_0 \cdot h(\xi), \quad A^* = A_0 \cdot A(\xi), \quad I^* = I_0 \cdot I(\xi), \tag{6}$$

where w_0, h_0, A_0 and I_0 are the reference width, thickness, cross-section area, and moment of inertia

$$A_0 = w_0 h_0, \quad I_0 = \frac{w_0 h_0^3}{12}, \tag{7}$$

considered at $x = 0$ regardless where the fixed end of the cantilever given by x_1 occurs; and w, h, A, and I are the dimensionless width, thickness, cross-section area, and moment of inertia, respectively

$$w(\xi) = 1, \quad h(\xi) = 1 - \xi^2, \quad A(\xi) = 1 - \xi^2, \quad I(\xi) = (1 - \xi^2)^3. \tag{8}$$

Differential equation (3) of transverse vibrations becomes in this case

$$\frac{1}{(1 - \xi^2)} \frac{d^2}{d\xi^2}\left[(1 - \xi^2)^3 \frac{d^2 Y}{d\xi^2}\right] - \bar{\omega}^2 Y = 0, \quad \xi \in [\xi_1, 1) \tag{9}$$

or

$$(1 - \xi^2)^2 \frac{d^4 Y}{d\xi^4} - 12\xi(1 - \xi^2)\frac{d^3 Y}{d\xi^3} - 6(1 - 5\xi^2)\frac{d^2 Y}{d\xi^2} - \bar{\omega}^2 Y = 0, \quad \xi \in [\xi_1, 1), \tag{10}$$

where the dimensionless coordinate ξ_1 of the fixed end, Fig. 1, can be anywhere between -1 and 1.

3.2. General solution

Eq. (10) can be factored as follows:

$$\left[(1-\xi^2)\frac{d^2}{d\xi^2} - 4\xi\frac{d}{d\xi} + \lambda_1\right] \cdot \left[(1-\xi^2)\frac{d^2}{d\xi^2} - 4\xi\frac{d}{d\xi} + \lambda_2\right] \cdot Y = 0, \tag{11}$$

where

$$\lambda_j = 2 + (-1)^j\sqrt{4 + \bar{\omega}^2}, \quad j = 1, 2. \tag{12}$$

Due to the factorization, solving the fourth order differential equation (10) reduces to solving the two second order differential equations which are given by Eq. (11). Using the variable changing

$$\xi = 1 - 2z, \tag{13}$$

the two second order differential equations given by Eq. (11) become

$$z(1-z)\frac{d^2Y}{dz^2} + [2 - 4z]\frac{dY}{dz} + \lambda_j Y = 0, \quad j = 1, 2. \tag{14}$$

Differential equations (14) are Gauss equations. As the canonical form of Gauss equation is

$$z(1-z)\frac{d^2y}{dz^2} + [c - (a + b + 1)z]\frac{dy}{dz} - aby = 0, \tag{15}$$

the Gauss coefficients, a_j, b_j, c_j of the two differential equations (14) are given by

$$\begin{cases} c_j = 2 \\ a_j + b_j = 3 \\ a_j b_j = -2 + (-1)^j\sqrt{4 + \bar{\omega}^2} \end{cases}, \quad j = 1, 2. \tag{16}$$

According to Abramovitz and Stegun (1965) the general solutions of the differential equations (14) are

$$Y_j(z) = A_j \cdot {_2F_1}(a_j, b_j, c_j, z) + B_j \cdot w_{j2}(z), \quad j = 1, 2, \tag{17}$$

where A_j, B_j, $j = 1,2$, are constants of integration, ${_2F_1}(a,b,c,z)$ is the hypergeometric function

$${_2F_1}(a, b, c, z) = \sum_{n=0}^{\infty} \frac{(a)_n (b)_n}{(c)_n} \frac{z^n}{n!}, \tag{18}$$

$w_{j2}(z)$ function is given by

$$w_{j2}(z) = {_2F_1}(a_j, b_i, c_j, z)\ln z + \sum_{n=1}^{\infty} \frac{(a_j)_n (b_j)_n}{n!(c_j)_n} z^n [\psi(a_j + n) - \psi(a_j) + \psi(b_j + n) - \psi(b_j) - \psi(n + c_j)$$

$$+ \psi(c_j) - \psi(n + 1) + \psi(1)] - \sum_{n=1}^{c_j - 1} \frac{(n-1)!(1 - c_j)_n}{(1 - a_j)_n (1 - b_j)_n} z^{-n}, \tag{19}$$

ψ is the logarithmic derivative of Gamma function Γ, and $(a)_n$ is the Pochhammer symbol or rising factorial

$$(a)_n = \frac{\Gamma(a + n)}{\Gamma(a)} = a(a + 1)\ldots(a + n - 1). \tag{20}$$

Since the second order differential operators of Eq. (11) are commuting operators, the general solution $Y(\xi)$ of Eq. (10) is a linear combination of the solutions $Y_1(\xi)$ and $Y_2(\xi)$, given by Eq. (17), as follows:

$$Y(\xi) = \sum_{j=1}^{2} \left[A_j \cdot {_2F_1}\left(a_j, b_j, c_j, \frac{1-\xi}{2}\right) + B_j \cdot w_{j2}\left(\frac{1-\xi}{2}\right)\right]. \tag{21}$$

The general solution given Eq. (21) holds for any beam of rectangular cross-section, constant width, and parabolic thickness variation, sharp or not, and any boundary conditions. Yet, only the case of sharp parabolic cantilevers is considered in what follows. Numerical determinations of the natural frequencies and mode shapes are presented in this case.

3.3. Boundary conditions and frequency equation of sharp parabolic cantilevers

Consider a parabolic cantilever with one end sharp. In this case both coefficients B_1 and B_2 of the general solution given by Eq. (21) must be zero, therefore the general solution in this case becomes

$$Y(\xi) = A_1 \cdot {}_2F_1\left(a_1, b_1, c_1, \frac{1-\xi}{2}\right) + A_2 \cdot {}_2F_1\left(a_2, b_2, c_2, \frac{1-\xi}{2}\right). \tag{22}$$

Both coefficients B_1 and B_2 must be zero because the functions $w_{j2}[(1-\xi)/2]$, $j = 1,2$, given by Eq. (19), become infinite at the sharp end, $\xi = 1$, due to the logarithmic function, and consequently the functions w_{j2}, $j = 1,2$, cannot be used since the transverse displacement of the cantilever must always remain finite. On the boundary $\xi = \xi_1$, the fixed end of the cantilever, the following conditions have to be met:

$$Y(\xi_1) = \frac{dY}{d\xi}(\xi_1) = 0. \tag{23}$$

Therefore the boundary value problem in the case of sharp cantilevers is given by Eqs. (22) and (23), and it leads to the following natural frequency equation:

$$F(\bar{\omega}^2) = \begin{vmatrix} {}_2F_1(a_1, b_1, c_1, \frac{1-\xi_1}{2}) & {}_2F_1\left(a_2, b_2, c_2, \frac{1-\xi_1}{2}\right) \\ a_1 b_1 \cdot {}_2F_1\left(a_1+1, b_1+1, c_1+1, \frac{1-\xi_1}{2}\right) & a_2 b_2 \cdot {}_2F_1\left(a_2+1, b_2+1, c_2+1, \frac{1-\xi_1}{2}\right) \end{vmatrix} = 0, \tag{24}$$

where coefficients a_j, b_j, c_j, $j = 1,2$ are given by Eq. (16). Solving Eq. (24), the dimensionless natural frequencies $\bar{\omega}_k$ are obtained. Denoting $a_{jk} = a_j(\bar{\omega}_k)$, $b_{jk} = b_j(\bar{\omega}_k)$, $j = 1,2$, the corresponding mode shapes $Y_k(\xi)$ result as

$$Y_k(\xi) = {}_2F_1\left(a_{1k}, b_{1k}, c_1, \frac{1-\xi}{2}\right) + D_k \cdot {}_2F_1\left(a_{2k}, b_{2k}, c_2, \frac{1-\xi}{2}\right), \tag{25}$$

where the coefficients D_k are given by

$$D_k = -\frac{{}_2F_1\left(a_{1k}, b_{1k}, c_1, \frac{1-\xi_1}{2}\right)}{{}_2F_1\left(a_{2k}, b_{2k}, c_2, \frac{1-\xi_1}{2}\right)}. \tag{26}$$

Few remarks regarding boundary conditions follow. First, if the free end of the cantilever was not sharp, i.e. it was a regular point of the differential equation, then the general solution of the equation of motion would be given by Eq. (21) and the free boundary conditions at this end would be those of zero bending moment and zero shear force. Second, at any sharp end, physically no specific displacement or slope can be enforced, so any sharp end must be a free end. Therefore no boundary such as pinned, fixed, or simply supported can occur at sharp ends. On the other hand, tacitly it is always required that the displacement and its derivatives are finite at every point of the cantilever. However, at the sharp end of the cantilever, $\xi = 1$, which is a singular point of the differential equation, the condition that the displacement is finite has to be explicitly enforced

$$Y(1) = \text{finite}. \tag{27}$$

Eq. (27) was the boundary condition that reduced Eq. (21) to Eq. (22). Third, the necessary condition of finite displacement at the sharp end, Eq. (27), Caruntu (2007), is a sufficient condition for zero bending moment and zero shear force (free boundary) in the case of parabolic sharp cantilever, see Appendix. This is consistent with the fact that a sharp end cannot sustain any moment or shear force. One can say that the usual boundary conditions of a free end, $M = T = 0$, zero bending moment and zero shear force, have to be replaced by $Y = \text{finite}$ at a sharp end. Fourth, the finite displacement condition, Eq. (27), eliminates from the general solution given by Eq. (21) the unbounded at $\xi = 1$ functions w_{j2}, $j = 1,2$, and leaves the general solution with only hypergeometric functions which are continuous and have continuous derivatives at $\xi = 1$.

3.4. Numerical determinations of exact modes

The exact natural modes, reported in what follows, are of sharp parabolic cantilevers of rectangular (or elliptical) cross-section. Eq. (24) has been solved using MATLAB (and MATHEMATICA) to find the first four natural frequencies for different values of the dimensionless coordinate of the fixed end, $\xi_1 = -1 + k/10$, where $k = 3, 4, \ldots, 17$. One can see from Fig. 1 that the cantilever dimensionless length is given by $1 - \xi_1$. Table 1 shows the first four natural frequencies of the beam and Fig. 2 graphs the first three natural frequencies. All the necessary coefficients for the corresponding mode shapes are given in Tables 2 and 3. The Gauss coefficients given by Eq. (16) are found in Table 2, and D coefficients given by Eq. (26) are found in

Table 1
First four natural frequencies $\bar{\omega} = \omega \ell^2 \sqrt{(\rho_0 A_0)/(EI_0)}$ of the cantilever given in Fig. 1 versus the dimensionless coordinate of the fixed end ξ_1

	ξ_1														
	−0.7	−0.6	−0.5	−0.4	−0.3	−0.2	−0.1	0	0.1	0.2	0.3	0.4	0.5	0.6	0.7
$\bar{\omega}_1$	1.050	1.469	1.936	2.465	3.070	3.770	4.593	5.576	6.772	8.263	10.17	12.72	16.27	21.60	30.47
$\bar{\omega}_2$	7.606	8.958	10.42	12.02	13.83	15.91	18.32	21.18	24.65	28.96	34.47	41.78	51.99	67.26	92.66
$\bar{\omega}_3$	18.25	20.91	23.79	26.96	30.54	34.63	39.40	45.05	51.90	60.41	71.29	85.72	105.9	136.0	186.2
$\bar{\omega}_4$	32.54	36.96	41.73	46.99	52.92	59.70	67.61	76.98	88.34	102.4	120.5	144.4	177.8	227.8	310.9
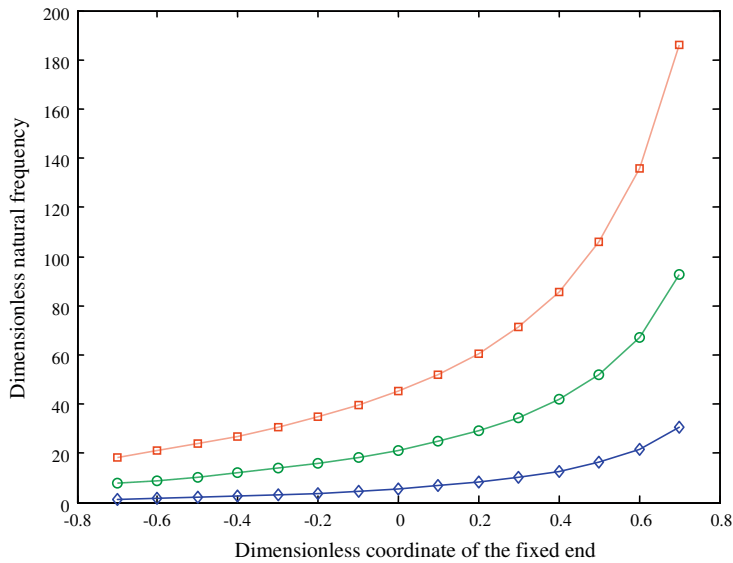
Fig. 2. First three dimensionless natural frequencies $\bar{\omega} = \omega \ell^2 \sqrt{(\rho_0 A_0)/(EI_0)}$ of the cantilever, Fig. 1, versus the coordinate ξ_1 of the fixed end; (——) first frequency, (----) second frequency, and (......) third frequency.

Table 2
Gauss coefficients a_{1k}, a_{2k} of the first four mode shapes $k = 1,2,3,4$ (see Eq. (25)) of the cantilever given in Fig. 1

		a_{11}	a_{21}	a_{12}	a_{22}	a_{13}	a_{23}	a_{14}	a_{24}
ξ_1	-0.7	4.051	2.911	4.981	$1.5 + 1.901i$	6.255	$1.5 + 3.756i$	7.571	$1.5 + 5.325i$
	-0.6	4.095	2.830	5.164	$1.5 + 2.220i$	6.526	$1.5 + 4.094i$	7.924	$1.5 + 5.724i$
	-0.5	4.152	2.711	5.354	$1.5 + 2.521i$	6.803	$1.5 + 4.430i$	8.284	$1.5 + 6.126i$
	-0.4	4.225	2.537	5.554	$1.5 + 2.818i$	7.094	$1.5 + 4.774i$	8.661	$1.5 + 6.541i$
	-0.3	4.313	2.266	5.769	$1.5 + 3.119i$	7.404	$1.5 + 5.134i$	9.064	$1.5 + 6.979i$
	-0.2	4.419	$1.5 + 0.1329i$	6.003	$1.5 + 3.432i$	7.740	$1.5 + 5.517i$	9.499	$1.5 + 7.449i$
	-0.1	4.543	$1.5 + 0.8715i$	6.262	$1.5 + 3.765i$	8.110	$1.5 + 5.933i$	9.979	$1.5 + 7.962i$
	0	4.690	$1.5 + 1.294i$	6.552	$1.5 + 4.126i$	8.525	$1.5 + 6.391i$	10.51	$1.5 + 8.530i$
	0.1	4.863	$1.5 + 1.677i$	6.884	$1.5 + 4.526i$	8.996	$1.5 + 6.906i$	11.12	$1.5 + 9.172i$
	0.2	5.071	$1.5 + 2.062i$	7.269	$1.5 + 4.978i$	9.543	$1.5 + 7.496i$	11.83	$1.5 + 9.910i$
	0.3	5.324	$1.5 + 2.474i$	7.727	$1.5 + 5.502i$	10.19	$1.5 + 8.190i$	12.67	$1.5 + 10.78i$
	0.4	5.638	$1.5 + 2.937i$	8.288	$1.5 + 6.130i$	10.99	$1.5 + 9.028i$	13.69	$1.5 + 11.84i$
	0.5	6.044	$1.5 + 3.485i$	9.002	$1.5 + 6.912i$	11.99	$1.5 + 10.08i$	14.99	$1.5 + 13.17i$
	0.6	6.594	$1.5 + 4.177i$	9.958	$1.5 + 7.940i$	13.34	$1.5 + 11.48i$	16.73	$1.5 + 14.95i$
	0.7	7.398	$1.5 + 5.127i$	11.35	$1.5 + 9.404i$	15.30	$1.5 + 13.49i$	19.25	$1.5 + 17.51i$

Table 3
Coefficients D_k of the first four mode shapes $k = 1,2,3,4$ (see Eq. (26)) of the cantilever given in Fig. 1

	ξ_1														
	-0.7	-0.6	-0.5	-0.4	-0.3	-0.2	-0.1	0	0.1	0.2	0.3	0.4	0.5	0.6	0.7
$D_1 \times 10^2$	45.25	33.83	25.41	19.30	14.86	11.62	9.219	7.424	6.060	5.009	4.187	3.537	3.016	2.593	2.247
$-D_2 \times 10^4$	75.11	55.87	43.51	34.99	28.82	24.19	20.61	17.78	15.50	13.64	12.09	10.79	9.695	8.754	7.943
$D_3 \times 10^6$	152.7	125.6	106.0	91.18	79.61	70.32	62.73	56.40	51.06	46.50	42.57	39.15	36.16	33.51	31.16
$-D_4 \times 10^7$	43.79	37.78	33.20	29.58	26.63	24.19	22.12	20.35	18.82	17.49	16.31	15.26	14.33	13.48	12.72

Table 3. For instance one can read for the case of $\xi_1 = 0$ that the second dimensionless natural frequency is $\bar{\omega}_2 = 21.18$ from Table 1, the Gauss coefficients for the corresponding mode shape given by Eq. (25) are $a_{12} = 6.552$ and $a_{22} = 1.5 + 4.126i$ from Table 2, and $D_2 = -17.78 \times 10^{-4}$ from Table 3. The coefficients $b_{12} = -3.552$ and $b_{22} = 1.5 - 4.126i$ result from Eq. (16). Therefore, for the case of $\xi_1 = 0$, the second dimensionless natural frequency and mode shapes are

$$\bar{\omega}_2 = 21.18, \tag{28}$$

$$Y_2(\xi) = {}_2F_1\left(6.552, -3.552, 2, \frac{1-\xi}{2}\right) - 17.78 \cdot 10^{-4} \cdot {}_2F_1\left(1.5 + 4.126i, 1.5 - 4.126i, 2, \frac{1-\xi}{2}\right). \tag{29}$$
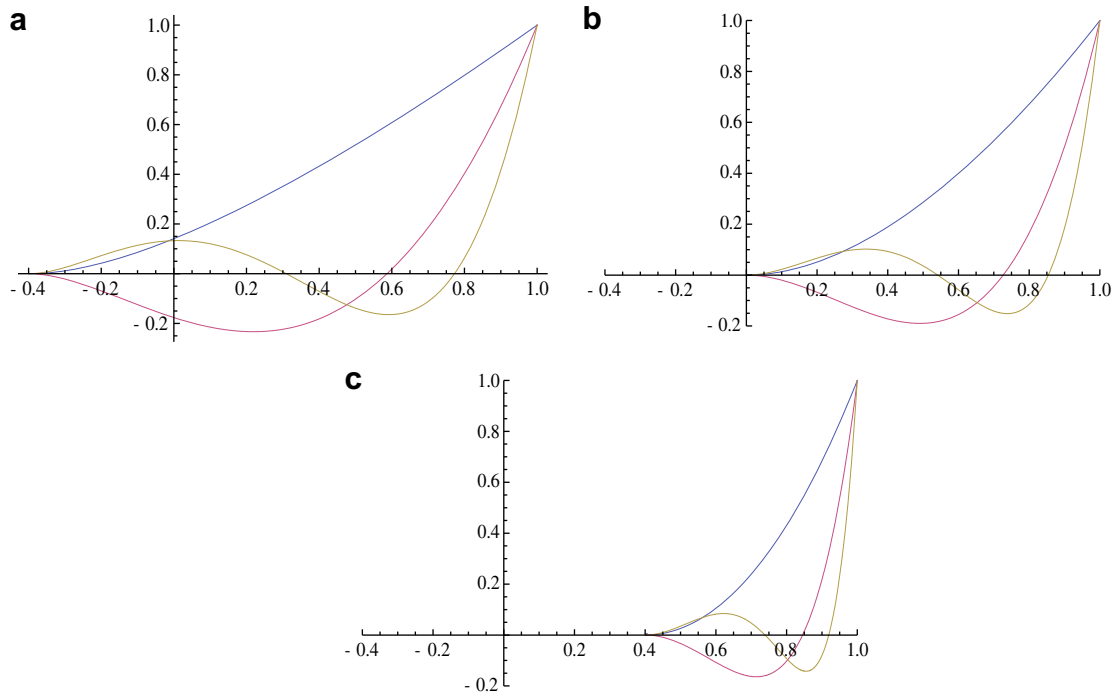
Fig. 3. First thee mode shapes of the cantilever given in Fig. 1 for three values of the dimensionless coordinate of the fixed end ξ_1: (a) $\xi_1 = -0.4$, (b) $\xi_1 = 0.0$, and (c) $\xi_1 = 0.4$.

Figure 3 shows the first three cantilever mode shapes for three different values of the dimensionless coordinates of the fixed end. One can use Fig. 1 to see the three geometry cases of the cantilever.

3.5. Approximate natural frequencies by Galerkin method

An approximate method, namely Galerkin method, is used to find approximations of the first two natural frequencies of transverse vibrations of a parabolic sharp cantilever whose fixed end is at $\xi_1 = 0$, Fig. 1, for comparison with the exact solutions reported in this paper. These approximations are shown to be close to the exact values reported in previous Section 3.4. The boundary value problem to be solved by Galerkin method is given by Eqs. (10) and (23). Look for a trial solution for the boundary value problem as follows

$$\bar{y}(\xi) = \sum_{i=1}^{2} b_i \varphi_i(\xi), \tag{30}$$

where $\varphi_i(\xi) = \xi^{i+1}$, and b_i are adjustable constants, $i = 1, 2$. One can see that the trial solution satisfies the boundary conditions given by Eq. (23) and is finite at $\xi = 1$. If $\bar{y}(\xi)$ was the true solution, then it would satisfy Eq. (10) identically. An approximate solution by Galerkin method is found from the requirement that the differential operator of Eq. (10) be orthogonal to the linear span of $\{\varphi_i\}$ which results into the following equations:

$$\int_0^1 \varphi_i(\xi) \left\{ (1 - \xi^2)^2 \frac{d^4 \bar{y}}{d\xi^4} - 12\xi(1 - \xi^2) \frac{d^3 \bar{y}}{d\xi^3} - 6(1 - 5\xi^2) \frac{d^2 \bar{y}}{d\xi^2} - \bar{\omega}^2 \bar{y} \right\} d\xi = 0, \quad i = 1, 2, \tag{31}$$

The constants b_i are determined from Eq. (31). After calculations the following algebraic system is obtained:

$$\begin{cases} b_1 \left(8.0 - \frac{\bar{\omega}^2}{5} \right) + b_2 \left(15.0 - \frac{\bar{\omega}^2}{6} \right) = 0, \\ b_1 \left(7.0 - \frac{\bar{\omega}^2}{6} \right) + b_2 \left(14.4 - \frac{\bar{\omega}^2}{7} \right) = 0. \end{cases} \tag{32}$$

This system of equations has nontrivial solutions if and only if its determinant is zero, which represents the eigenvalue equation. Solving this equation, the approximate values of the first two natural frequencies are found to be 5.54 and 20.44. These values are close to the exact values of 5.576 and 21.18 given in Table 1.

4. Beams of circular cross-section and parabolic radius variation

4.1. Differential equation

Consider a beam of circular cross-section of parabolic radius variation, Fig. 4. The current radius $R^*(x)$ is given by

$$R^*(x) = R_0\left(1 - \frac{x^2}{\ell^2}\right), \quad x_1 < x < \ell. \tag{33}$$

Using the variable changing given by Eq. (2), the current radius R^*, cross-section area A^*, and moment of inertia I^* can be written as

$$R^* = R_0 \cdot R(\xi), \quad A^* = A_0 \cdot A(\xi), \quad I^* = I_0 \cdot I(\xi), \tag{34}$$

where R_0, A_0, and I_0 are the reference (at $x = 0$) radius, cross-section area, and moment of inertia, respectively

$$A_0 = \pi R_0^2, \quad I_0 = \frac{\pi R_0^4}{4}, \tag{35}$$

and R, A, I are the dimensionless radius, cross-section area, and moment of inertia, respectively

$$R(\xi) = (1 - \xi^2), \quad A(\xi) = (1 - \xi^2)^2, \quad I(\xi) = (1 - \xi^2)^4. \tag{36}$$

The self-adjoint differential equation (3) becomes

$$\frac{1}{(1-\xi^2)^2}\frac{d^2}{d\xi^2}\left[(1-\xi^2)^4\frac{d^2Y}{d\xi^2}\right] - \bar{\omega}^2 Y = 0, \quad \xi \in [\xi_1, 1), \quad \xi_1 \in (-1, 1), \tag{37}$$

or in its expanded form

$$(1-\xi^2)^2\frac{d^4Y}{d\xi^4} - 16\xi(1-\xi^2)\frac{d^3Y}{d\xi^3} - 8(1-7\xi^2)\frac{d^2Y}{d\xi^2} - \bar{\omega}^2 Y = 0. \tag{38}$$

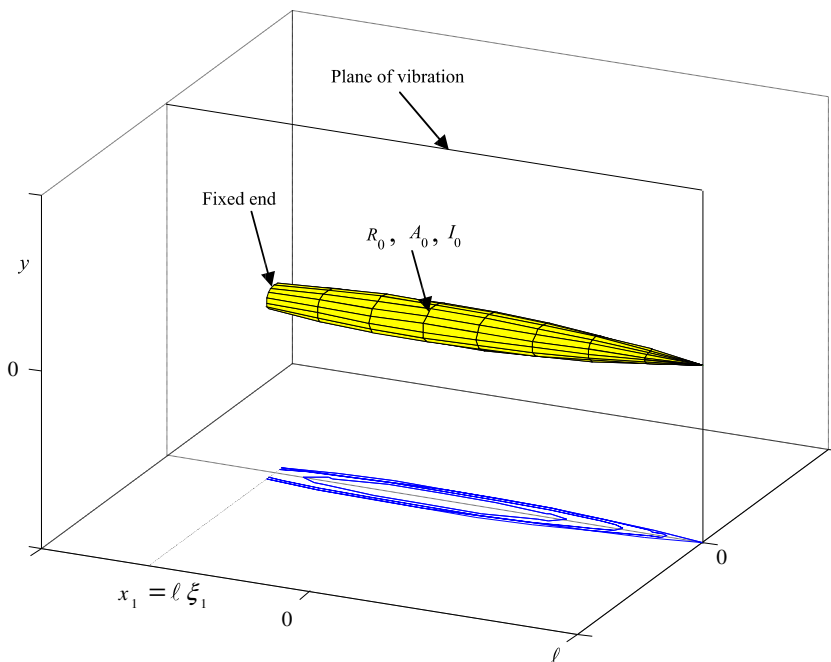### 4.2. General solution, boundary, and frequency equation

Eq. (38) can be factored as

Fig. 4. Cantilever of circular cross-section, parabolic radius variation $R^* = R_0(1 - \xi^2)$, and sharp end.

$$\left[(1-\xi^2)\frac{d^2}{d\xi^2} - 6\xi\frac{d}{d\xi} + \lambda_1\right] \cdot \left[(1-\xi^2)\frac{d^2}{d\xi^2} - 6\xi\frac{d}{d\xi} + \lambda_2\right] \cdot Y = 0, \tag{39}$$

where

$$\lambda_j = 3 + (-1)^j\sqrt{9 + \bar{\omega}^2}, \quad j = 1, 2. \tag{40}$$

Using the variable changing given by Eq. (13), the two second order differential equations of the factored equation (39) become Gauss differential equations with coefficients a_j, b_j, c_j given by

$$\begin{cases} c_j = 3 \\ a_j + b_j = 5 \\ a_jb_j = -3 + (-1)^j\sqrt{9 + \bar{\omega}^2} \end{cases}, \quad j = 1, 2. \tag{41}$$

The general solution given by Eqs. (21) and (41) holds for any boundary conditions of parabolic cantilevers of circular cross-section. Eqs. (22) and (24) are the general solution and the frequency equation, respectively, of the boundary value problem of sharp parabolic cantilevers given by Eqs. (38) and (23), where the coefficients a_j, b_j, c_j are given by Eq. (41). The mode shapes are given by Eqs. (25) and (41). Yet, only sharp parabolic cantilever case is considered for numerical determinations.

4.3. Numerical determinations of exact modes

The exact natural modes, reported in what follows, are of sharp parabolic cantilevers of circular cross-section. Eq. (24) with Gauss coefficients given by Eq. (41) has been solved using MATLAB (and MATHEMATICA) for finding the first four natural frequencies. Different values of the dimensionless coordinate of the fixed end, $\xi_1 = -1 + k/10$, where $k = 3, 4, \ldots, 17$, were considered. Table 4 shows the first four natural frequencies of the beam. Fig. 5 graphs the first three natural frequencies. All the necessary coefficients for the first four corresponding mode shapes are given in Tables 5 and 6. The Gauss coefficients are given in Table 5, and the D coefficients given by Eq. (26) are found in Table 6. For instance one can read for the case of $\xi_1 = 0$

Table 4
First four natural frequencies $\bar{\omega} = \omega\ell^2\sqrt{(\rho_0A_0)/(EI_0)}$ of the cantilever given in Fig. 4 versus the dimensionless coordinate of the fixed end ξ_1

	ξ_1														
	−0.7	−0.6	−0.5	−0.4	−0.3	−0.2	−0.1	0	0.1	0.2	0.3	0.4	0.5	0.6	0.7
$\bar{\omega}_1$	1.011	1.572	2.238	3.020	3.940	5.026	6.322	7.886	9.805	12.21	15.31	19.45	25.26	33.97	48.49
$\bar{\omega}_2$	8.727	10.57	12.55	14.75	17.23	20.07	23.40	27.35	32.15	38.12	45.75	55.90	70.07	91.29	126.6
$\bar{\omega}_3$	21.25	24.49	28.12	32.14	36.68	41.88	47.96	55.18	63.93	74.80	88.71	107.2	133.0	171.6	235.8
$\bar{\omega}_4$	37.25	42.54	48.29	54.66	61.84	70.07	79.68	91.09	104.9	122.1	144.0	173.2	213.9	274.8	376.2
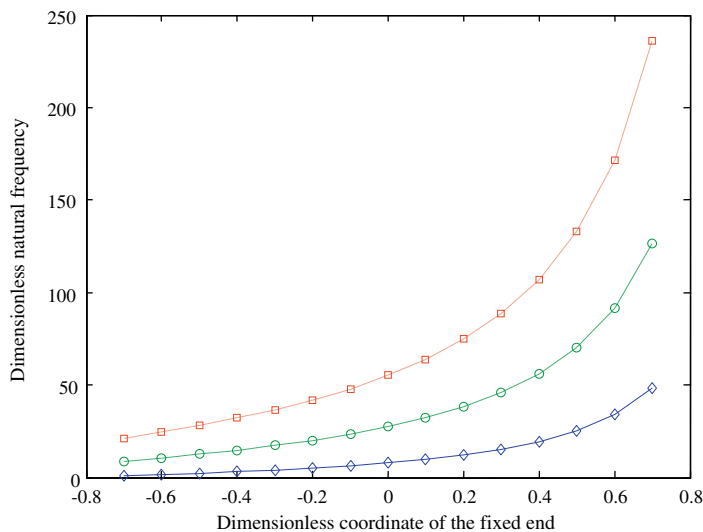
Fig. 5. First three dimensionless natural frequencies $\bar{\omega} = \omega\ell^2\sqrt{(\rho_0A_0)/(EI_0)}$ of the cantilever, Fig. 4, versus the coordinate ξ_1 of the fixed end; (——) first frequency, (- - - -) second frequency, (. . .dots) third frequency.

Table 5
Gauss coefficients a_{1k}, a_{2k} of the first four mode shapes $k = 1,2,3,4$ (see Eq. (25)) of the cantilever given in Fig. 4

ξ_1	a_{11}	a_{21}	a_{12}	a_{22}	a_{13}	a_{23}	a_{14}	a_{24}
−0.7	6.024	4.967	6.799	2.649	8.033	2.5 + 3.480i	9.328	2.5 + 5.303i
−0.6	6.055	4.921	6.998	2.5 + 1.317i	8.324	2.5 + 3.927i	9.704	2.5 + 5.780i
−0.5	6.105	4.847	7.207	2.5 + 1.912i	8.626	2.5 + 4.362i	10.09	2.5 + 6.256i
−0.4	6.175	4.735	7.429	2.5 + 2.408i	8.944	2.5 + 4.799i	10.50	2.5 + 6.744i
−0.3	6.269	4.573	7.671	2.5 + 2.870i	9.286	2.5 + 5.249i	10.94	2.5 + 7.257i
−0.2	6.386	4.343	7.936	2.5 + 3.324i	9.658	2.5 + 5.722i	11.41	2.5 + 7.803i
−0.1	6.531	4.001	8.231	2.5 + 3.787i	10.07	2.5 + 6.229i	11.93	2.5 + 8.396i
0	6.706	3.402	8.564	2.5 + 4.274i	10.53	2.5 + 6.783i	12.52	2.5 + 9.049i
0.1	6.916	2.5 + 1.002i	8.945	2.5 + 4.800i	11.06	2.5 + 7.400i	13.19	2.5 + 9.783i
0.2	7.172	2.5 + 1.824i	9.391	2.5 + 5.384i	11.67	2.5 + 8.100i	13.96	2.5 + 10.62i
0.3	7.485	2.5 + 2.521i	9.923	2.5 + 6.050i	12.40	2.5 + 8.9173i	14.88	2.5 + 11.61i
0.4	7.879	2.5 + 3.230i	10.58	2.5 + 6.836i	13.29	2.5 + 9.899i	16.01	2.5 + 12.81i
0.5	8.389	2.5 + 4.023i	11.41	2.5 + 7.803i	14.43	2.5 + 11.12i	17.44	2.5 + 14.31i
0.6	9.084	2.5 + 4.985i	12.53	2.5 + 9.060i	15.95	2.5 + 12.74i	19.36	2.5 + 16.30i
0.7	10.11	2.5 + 6.272i	14.16	2.5 + 10.83i	18.15	2.5 + 15.05i	22.13	2.5 + 19.16i

Table 6
Coefficients D_k of the first four mode shapes $k = 1,2,3,4$ (see Eq. (26)) of the cantilever given in Fig. 4

	ξ_1													
	−0.7	−0.6	−0.5	−0.4	−0.3	−0.2	−0.1	0	0.1	0.2	0.3	0.4	0.5	0.6	0.7
$D_1 \times 10^2$	50.88	37.14	26.45	18.64	13.17	9.397	6.809	5.019	3.765	2.871	2.224	1.748	1.392	1.122	0.914
$-D_2 \times 10^4$	81.11	52.72	36.40	26.25	19.57	14.98	11.72	9.332	7.549	6.188	5.132	4.300	3.637	3.101	2.663
$D_3 \times 10^6$	113.6	86.18	67.02	53.26	43.10	35.42	29.50	24.86	21.16	18.17	15.73	13.71	12.03	10.62	9.417
$D_4 \times 10^7$	26.07	21.19	17.46	14.59	12.35	10.57	9.128	7.953	6.981	6.170	5.485	4.903	4.403	3.973	3.599

that the second dimensionless natural frequency is $\bar{\omega}_2 = 27.35$, and the coefficients for the corresponding mode shape given by Eq. (25) are $a_{12} = 8.564$ and $a_{22} = 2.5 + 4.274i$ from Table 2, and $D_2 = -9.332 \times 10^{-4}$ from Table 3. The coefficients $b_{12} = -3.564$ and $b_{22} = 2.5 - 4.274i$ result from Eq. (41). Therefore, for the case of $\xi_1 = 0$, the second dimensionless natural frequency and mode shapes are

$$\bar{\omega}_2 = 27.35, \tag{42}$$

$$Y_2(\xi) = {}_2F_1\left(8.564, -3.564, 3, \frac{1-\xi}{2}\right) - 9.332 \cdot 10^{-4} \cdot {}_2F_1\left(2.5 + 4.274i, 2.5 - 4.274i, 3, \frac{1-\xi}{2}\right). \tag{43}$$

5. Modal characteristics in terms of fixed end cross-section and total length

This section provides the way of expressing the results reported in this paper in terms of fixed end cross-section characteristics and total length of the cantilever, and shows that as the parabolic thickness profile approaches the linear profile so do the dimensionless natural frequencies. To express the results in terms of fixed end geometrical characteristics and total length of the cantilever Eq. (1) is written in terms of a new independent variable $\tilde{x}$ resulted from a translation of the x coordinate system to the fixed end by x_1

$$\tilde{x} = x - x_1, \quad 0 < \tilde{x} < L \tag{44}$$

$$L = \ell - x_1, \quad \tilde{x}_0 = -x_1, \tag{45}$$

where L is the total length of the cantilever, ℓ is half of the complete beam (sharp at both ends), x_1 is the coordinate of the fixed end on the x axis (see Fig. 1), and $\tilde{x}_0$ is the $\tilde{x}$ coordinate of the origin of x axis. The origin of x axis was taken as the midpoint of the complete beam, the point where the complete beam has its maximum thickness. Eq. (1) in variable x and Eq. (1) in variable $\tilde{x}$ are equivalent, so one can use the results in x for finding the ones in $\tilde{x}$. Denote the dimensionless coordinate corresponding to $\tilde{x}$ by η. Therefore

$$\eta = \frac{\tilde{x}}{L}, \quad 0 < \eta < 1. \tag{46}$$

Using Eqs. (44) and (2) the relationship between the two dimensionless coordinates η and ξ corresponding to x and $\tilde{x}$ coordinates, respectively, is

$$\xi = \frac{\eta - \gamma}{1 - \gamma}, \quad \gamma = \frac{\tilde{x}_0}{L}, \tag{47}$$

where the geometric parameter γ indicates the dimensionless location of the midpoint of the complete beam with respect to the fixed end of the actual beam. For instance in Fig. 1 the midpoint of the complete beam is a real point on the actual beam and it is on the positive $\tilde{x}$ axis whose origin is at the fixed end. Consequently $\tilde{x}_0$ is positive and less than L, so γ is positive and less than one. If the midpoint of the complete beam was on the negative $\tilde{x}$ axis then it would have not been a real point of the actual beam, and γ would have been negative. The larger the absolute value of the negative γ the closer the parabolic variation to a linear variation. Using Eq. (47) the mode shapes given by Eq. (25) become

$$Y_k(\xi) = {}_2F_1(a_{1k}, b_{1k}, c_1, \frac{1-\eta}{2(1-\gamma)}) + D_k \cdot {}_2F_1\left(a_{2k}, b_{2k}, c_2, \frac{1-\eta}{2(1-\gamma)}\right), \quad 0 < \eta < 1 \tag{48}$$

The dimensionless natural frequencies $\tilde{\omega}_k$ in terms of the geometrical characteristics of the fixed end cross-section given by

$$\tilde{\omega} = \omega L^2 \sqrt{\frac{\rho_0 A_1}{EI_1}}, \tag{49}$$

can be found from the dimensionless natural frequency $\bar{\omega}$, given in terms of the geometrical characteristics of the cross-section at the midpoint of the complete beam, as follows:

$$\tilde{\omega} = \frac{\bar{\omega}}{(1-2\gamma)}, \tag{50}$$

where A_1 and I_1 are cross-section area and moment of inertia at the fixed end. The relationship between ξ_1 and parameter γ is obtained from Eq. (47) as follows

$$\xi_1 = \frac{-\gamma}{1-\gamma}, \tag{51}$$

since at the fixed end $\xi = \xi_1$ and $\eta = 0$. The intervals for the two parameters are $\xi_1 \in (-1, 1)$ and $\gamma \in (-\infty, 0.5)$. One can find $\tilde{\omega}$ using Tables 1 and 2 as follows. For instance to find $\tilde{\omega}_1$ corresponding to $\bar{\omega}_1 = 8.263$ and $\xi_1 = 0.2$, from Table 1, one uses Eqs. (51) and (50) and finds $\gamma = -0.25$ and $\tilde{\omega}_1 = 5.509$, respectively.

An interesting remark is that for $\xi_1 = 0$, $\xi_1 = 0.2$, $\xi_1 = 0.5$, and $\xi_1 = 0.7$ for which Table 1 provides $\bar{\omega}_1 = 5.576$, $\bar{\omega}_1 = 8.263$, $\bar{\omega}_1 = 16.27$, and $\bar{\omega}_1 = 30.47$, respectively, one determines $\gamma = 0$, $\gamma = -0.25$, $\gamma = -1$, and $\gamma = -2.\bar{3}$, and the frequencies $\tilde{\omega}$ result as $\tilde{\omega}_1 = 5.576$, $\tilde{\omega}_1 = 5.509$, $\tilde{\omega}_1 = 5.423$, and $\tilde{\omega}_1 = 5.377$, respectively. This is in good agreement with data reported in the literature since as γ, given by Eq. (47), decreases from zero, the parabolic thickness profile approaches the linear thickness profile and the values of the dimensionless natural frequencies $\tilde{\omega}_1$ approach the value of $\bar{\omega}_1 = 5.31$ which was reported by Cranch and Adler (1956) as being the dimensionless natural frequency of linear thickness cantilevers. To see that as γ decreases from zero the parabolic thickness profile approaches a linear profile, one can find from dimensionless thickness h expressed in terms of η

$$h(\eta) = (1-\eta)\left(1 + \frac{1}{1-2\gamma}\eta\right) \tag{52}$$

the slope of dimensionless thickness h at the fixed end, $\eta = 0$, as follows:

$$h'(0) = -1 + \frac{1}{1-2\gamma}. \tag{53}$$

For the values of $\gamma = 0$, $\gamma = -0.25$, $\gamma = -1$, and $\gamma = -2.\bar{3}$, the following values of dimensionless thickness slopes at the fixed end are obtained 0.0, $-0.\bar{3}$, $-0.\bar{6}$, -0.82. These values approach -1 which is the dimensionless thickness slope of cantilevers of linear thickness.

6. Discussion and conclusions

Numerous investigators reported transverse vibrations of nonuniform structural elements. They used either analytical or approximate methods. Yet, closed-form analytical solutions were found only for few classes of nonuniform beams. Other solutions than those reported in this work were reported in terms of orthogonal polynomials, Bessel functions, or power series by Frobenius method. This paper presented the general solution in terms of hypergeometric functions and the exact modal characteristics for transverse vibrations of sharp cantilevers of parabolic variation in two cases, rectangular cross-section and circular cross-section. Free transverse vibrations in one principal plane developed on the Euler–Bernoulli hypothesis were considered. The beam geometry considered in this paper consisted of constant width and parabolic thickness variation if rectangular cross-section, and parabolic radius variation if circular cross-section. The results reported in this work for cantilevers of rectangular cross-section can also be used for corresponding cantilevers of elliptical cross-section. The reference cross-section area and reference moment of inertia given by Eq. (7) have to change to those of elliptical cross-section, although.

This paper is relevant in a few aspects. It reports the exact mode shapes and the natural frequencies of parabolic cantilevers which are next to the linear cantilevers as nonuniform geometry. These exact mode shapes and natural frequencies

can be used (1) as a source of basic design for situations which happen to fall within the geometry and boundary conditions presented here, (2) for studying forced and nonlinear vibrations of these cantilevers, and (3) as test cases for the development of numerical methods. The mode shapes can be used (4) as admissible functions for approximate methods as well. In general exact mode shapes and natural frequencies have the advantage of being of great ease for further use. In particular, hypergeometric functions, which are exact mode shapes in this work, are versatile tools. They are included as special mathematical functions in very popular commercial software packages such as MAPLE, MATHEMATICA, and MATLAB. Also, their mathematical properties are well developed Abramovitz and Stegun (1965). The results of this paper are limited to Euler-Bernoulli cantilevers, i.e. they are not accurate in the case of short cantilevers.

Appendix

This shows that the necessary condition of finite displacement at the sharp end, Eq. (27), is also a sufficient condition for free boundary, leading to zero bending moment and zero shear force. Two propositions follow. The first proposition shows that in general if a function is continuous on an interval closed at one end, so finite at this end, and its derivatives are continuous on the open interval, then these are sufficient conditions for the existence of the limits at this end of certain functions involving function's derivatives. The second proposition shows that using proposition one zero bending moment and zero shear force at a sharp end of a parabolic cantilever result. Lagrange's theorem is used to prove proposition one. Lagrange's theorem states that if a function $y(x)$ is continuous in a closed interval $[a,b]$, and differentiable in the open interval (a,b), then there is a c value in (a,b) such that

$$y'(c) = \frac{y(b) - y(a)}{b - a}, \tag{54}$$

where $' = dy/dx$. Without loss of generality consider $b = 1$.

Proposition 1. *Given a function $y(x)$, continuous on an interval closed at one end $(a, 1]$ and its first three derivatives continuous on the open interval $(a, 1)$ then*

$$\lim_{x \to 1}(1 - x)^n y^{(n)}(x) = 0, \quad n = 1, 2, 3. \tag{55}$$

Proof. Due to continuity of function $y(x)$ at $x = 1$, $y(1)$ exists and it is finite. According to Lagrange's theorem there is a c value such that

$$y(1) - y(x) = y'(c)(1 - x), \quad x < c < 1. \quad \square \tag{56}$$

Thus, using the triangle inequality, it results

$$|y(1) - y(x)| = |y'(c)(1 - x)| \geqslant |y'(c)(1 - c)| \geqslant 0. \tag{57}$$

If $x \to 1$, then $c \to 1$, and $|y(1) - y(x)| \to 0$ due to continuity at $x = 1$ of the function $y(x)$. Therefore

$$0 \geqslant \lim_{c \to 1}|y'(c)(1 - c)| \geqslant 0 \tag{58}$$

and consequently, using x instead of c, the case of $n = 1$ of the proposition is obtained

$$\lim_{x \to 1}(1 - x)y'(x) = 0. \tag{59}$$

In the case of $n = 2$, using Lagrange's theorem for the function $g(x) = (1 - x)y'(x)$.

$$g(1) - g(x) = g'(c)(1 - x), \quad x < c < 1. \tag{60}$$

It results

$$-y'(x) = (1 - c)y''(c) - y'(c), \quad x < c < 1. \tag{61}$$

Multiplying by $(1 - c)$ and rearranging terms, Eq. (61) becomes

$$-(1 - c)y'(x) + (1 - c)y'(c) = (1 - c)^2 y''(c). \tag{62}$$

Using the triangle inequality the following is obtained:

$$|(1 - x)y'(x)| + |(1 - c)y'(c)| \geqslant |-(1 - c)y'(x) + (1 - c)y'(c)| = |(1 - c)^2 y''(c)| \geqslant 0. \tag{63}$$

If $x \to 1$, then $c \to 1$, and both $|(1 - x)y'(x)| \to 0$ and $|(1 - c)y'(c)| \to 0$ due to case $n = 1$ of the proposition. Therefore

$$0 \geqslant \lim_{c \to 1}|(1 - c)^2 y''(c)| \geqslant 0. \tag{64}$$

Consequently, using x instead of c, the case of $n = 2$ of the proposition is obtained

$$\lim_{x \to 1}(1 - x)^2 y''(x) = 0. \tag{65}$$

In the case of $n = 3$, using Lagrange's theorem for function $h(x) = (1 - x)^2 y''(x)$

$$h(1) - h(x) = h'(c)(1 - x), \quad x < c < 1 \tag{66}$$

it results

$$-(1 - x)y''(x) = (1 - c)^2 y'''(c) - 2c(1 - c)y''(c), \quad x < c < 1. \tag{67}$$

Multiplying by $(1 - c)$ and rearranging terms it results

$$-(1 - c)(1 - x)y''(x) + 2c(1 - c)^2 y''(c) = (1 - c)^3 y'''(c). \tag{68}$$

Using the triangle inequality, the following inequalities can be written as

$$|(1 - x)^2 y''(x)| + |2c(1 - c)^2 y''(c)| \geqslant |-(1 - x)(1 - c)y''(x) + 2c(1 - c)^2 y''(c)| = |(1 - c)^3 y'''(c)| \geqslant 0. \tag{69}$$

If $x \to 1$, then $c \to 1$, and both $|(1 - x)^2 y''(x)| \to 0$ and $|(1 - c)^2 y'(c)| \to 0$ due to case $n = 2$ of the proposition. Therefore

$$0 \geqslant \lim_{c \to 1} |(1 - c)^3 y'''(c)| \geqslant 0. \tag{70}$$

Consequently, using x instead of c, the case of $n = 3$ of the proposition is obtained

$$\lim_{x \to 1}(1 - x)^3 y'''(x) = 0. \tag{71}$$

Proposition 2. *The necessary condition of finite displacement $Y(\xi)$ at the sharp end, $\xi = 1$, is a sufficient condition for free boundary (zero bending moment and zero shear force) at this end for beams of parabolic thickness.*

Proof. In general, the dimensionless bending moment $M(\xi)$ and shear force $T(\xi)$ are given by

$$M(\xi) = I(\xi)\frac{d^2 y(\xi)}{d\xi^2}, \quad T(\xi) = \frac{dM(\xi)}{d\xi}. \quad \square \tag{72}$$

In the case of parabolic thickness variation, Eq. (72) become

$$M(\xi) = (1 - \xi^2)^3 \frac{d^2 y(\xi)}{d\xi^2}, \tag{73}$$

$$T(\xi) = (1 - \xi^2)^3 \frac{d^3 y(\xi)}{d\xi^3} - 6\xi(1 - \xi^2)^2 \frac{d^2 y(\xi)}{d\xi^2} \tag{74}$$

by using the dimensionless cross-section moment of inertia $I(\xi)$, Eq. (8). Using Proposition 1, the bending moment at the sharp end is found to be zero

$$\lim_{\xi \to 1} M(\xi) = \lim_{\xi \to 1}(1 + \xi)^3 \lim_{\xi \to 1}(1 - \xi) \cdot \left[\lim_{\xi \to 1}(1 - \xi)^2 y''(\xi)\right] = 0. \tag{75}$$

Analogously, the shear force at the sharp end is found to be zero

$$\lim_{\xi \to 1} T(\xi) = \lim_{\xi \to 1}(1 + \xi)^3 \cdot \left[\lim_{\xi \to 1}(1 - \xi)^3 y'''(\xi)\right] - \lim_{\xi \to 1} 6\xi(1 + \xi)^2 \cdot \left[\lim_{\xi \to 1}(1 - \xi)^2 y''(\xi)\right] = 0. \tag{76}$$

Remark. Another way to prove Proposition 2 without using Proposition 1 is the following. In the case of general solution given by Eq. (21), as mentioned in the last paragraph of Section 3.3, the finite displacement at the sharp end condition eliminates the unbounded at $\xi = 1$ functions $w_{j2}, j = 1, 2$, and leaves the general solution with only hypergeometric functions which are continuous and have continuous derivatives at $\xi = 1$. This way, because $d^2 y(\xi)/d\xi^2$ and $d^3 y(\xi)/d\xi^3$ are finite at $\xi = 1$, according to Eqs. (73) and (74), both the bending moment and shear force vanish at $\xi = 1$.

References

Abramovitz, M., Stegun, I., 1965. Handbook of Mathematical Functions. Dover, New York.

Abrate, S., 1995. Vibration of nonuniform rods and beams. Journal of Sound and Vibration 185 (4), 703–716.

Anderson, D.R., Hoffacker, J., 2006. Existence of solutions for a cantilever beam problem. Journal of Mathematical Analysis and Applications 323, 958–973.

Auciello, N.M., Nole, G., 1998. Vibrations of a cantilever tapered beam with varying section properties and carrying a mass at the free end. Journal of Sound and Vibration 214 (1), 105–119.

Caruntu, D.I., 2007. Classical Jacobi polynomials, closed-form solutions for transverse vibrations. Journal of Sound and Vibration 306 (3–5), 467–494.

Caruntu, D.I., 2005. Self-adjoint differential equation for classical orthogonal polynomials. Journal of Computational and Applied Mathematics 180 (1), 107–118.

Caruntu, D.I., 1996. On bending vibrations of some kinds of beams of variable cross-section using orthogonal polynomials. Revue Roumaine des Sciences Techniques. Série de Mécanique Appliquée 41 (3–4), 265–272.

Chaudhari, T.D., Maiti, S.K., 1999. Modeling of transverse vibration of beam of linearly variable depth with edge crack. Engineering Fracture Mechanics 63, 425–445.

Cimalla, V., Niebelschutz, F., Tonisch, K., Foerster, C.H., Brueckner, K., Cimalla, I., Friedrich, T., Pezoldt, J., Stephan, R., Hein, M., Ambachera, O., 2007. Nanoelectromechanical devices for sensing applications. Sensors and Actuators B 126, 24–34.

Conway, H.D., Dubil, J.F., 1965. Vibration frequencies of truncated wedge and cone beam. Journal of Applied Mechanics 32E, 932–935.

Conway, H.D., Becker, E.C.H., Dubil, J.F., 1964. Vibration frequencies of tapered bars and circular plates. Journal of Applied Mechanics, 329–331.

Cranch, E.T., Adler, A., 1956. Bending vibrations of variable section beams. Journal of Applied Mechanics, 103–108.

Craver Jr., W.L., Jampala, P., 1993. Transverse vibrations of a linearly tapered cantilever beam with constraining springs. Journal of Sound and Vibration 166 (3), 521–529.

De Rosa, M.A., Auciello, N.M., 1996. Free vibrations of tapered beams with flexible ends. Computers and Structures 60 (2), 197–202.

Ece, M.C., Aydogdu, M., Taskin, V., 2007. Vibration of a variable cross-section beam. Mechanics Research Communications 34, 78–84.

Firouz-Abadi, R.D., Haddadpour, H., Novinzadeh, A.B., 2007. An asymptotic solution to transverse free vibrations of variable-section beams. Journal of Sound and Vibration 304 (3–5), 530–540.

Goel, R.P., 1976. Transverse vibration of tapered beams. Journal of Sound and Vibration 47 (1), 1–7.

Johnson, L., Gupta, A.K., Ghafoor, A., Akin, D., Bashir, R., 2006. Characterization of vaccinia virus particles using microscale silicon cantilever resonators and atomic force microscopy. Sensors and Actuators B 115, 189–197.

Mabie, J.J., Rogers, C.B., 1968. Traverse vibrations of tapered cantilever beams with end support. Journal of Acoustical Society of America 44, 1739–1741.

Naguleswaran, S., 1995. The vibration of a "complete" Euler–Bernoulli beam of constant depth and breadth proportional to axial co-ordinate raised to a positive exponents. Journal of Sound and Vibration 187 (2), 311–327.

Naguleswaran, S., 1994a. Vibration in the two principal planes of a nonuniform beam of rectangular cross-section, one side of which varies as the square root of the axial co-ordinate. Journal of Sound and Vibration 172 (3), 305–319.

Naguleswaran, S., 1994b. A direct solution for the transverse vibration of Euler–Bernoulli wedge and cone beams. Journal of Sound and Vibration 172 (3), 289–304.

Rao, S.S., 2004. Mechanical Vibrations, fourth ed. Person Prentice Hall.

Sanger, D.J., 1968. Transverse vibration of a class of nonuniform beams. Journal of Mechanical Engineering Science 16, 111–120.

Storti, D., Aboelnaga, Y., 1987. Bending vibrations of a class of rotating beams with hypergeometric solutions. Journal of Applied Mechanics 54, 311–314.

Timoshenko, S., Young, D.H., Weaver Jr., W., 1974. Vibration Problems in Engineering, fourth ed. John Wiley & Sons, New York.

Turner, J.A., Wiehn, J.S., 2001. Sensitivity of flexural and torsional vibration modes of atomic force microscope cantilevers to surface stiffness variations. Nanotechnology 12, 322–330.

Wang, H.C., 1967. Generalized hypergeometric function solutions on the transverse vibrations of a class of nonuniform beams. Journal of Applied Mechanics 34E, 702–708.

Wright, A.D., Smith, C.E., Thresher, R.W., Wang, J.L.C., 1982. Vibration modes of centrifugally stiffened beam. Journal of Applied Mechanics 49, 197–202.